Inorg. Chem. **2002**, *41*, 2219–2228

Synthesis and Structural Characterization of Trinuclear Cu^{II}–Pyrazolato Complexes Containing μ_3-OH, μ_3-O, and μ_3-Cl Ligands. Magnetic Susceptibility Study of $[PPN]_2[(\mu_3\text{-}O)Cu_3(\mu\text{-}pz)_3Cl_3]$

Panagiotis A. Angaridis,[+] Peter Baran,[§] R. Boča,*[,‡] Francisco Cervantes-Lee,[†] W. Haase,[#] Gellert Mezei,[§] Raphael G. Raptis,*[,§] and R. Werner[#]

Department of Chemistry, University of Puerto Rico, P.O. Box 23346, San Juan, Puerto Rico 00931-3346, Department of Inorganic Chemistry, Slovak Technical University, SK-812 37, Bratislava, Slovakia, Department of Chemistry, University of Texas at El Paso, El Paso, Texas 79968, and Institute of Physical Chemistry, Darmstadt University of Technology, Darmstadt, Germany

Received June 25, 2001

The nine-membered $[-Cu^{II}-N-N-]_3$ ring of trimeric copper–pyrazolato complexes provides a sturdy framework on which water is twice deprotonated in consecutive steps, forming μ_3-OH and μ_3-O species. In the presence of excess chlorides the μ_3-O(H) ligand is replaced by two μ_3-Cl ions. The interconversion of μ_3-OH and μ_3-O and the exchange of μ_3-O(H) and μ_3-Cl are reversible, and the three species involved have been structurally characterized: $[PPN][Cu_3(\mu_3\text{-}OH)(\mu\text{-}pz)_3Cl_3(thf)]\cdot CH_2Cl_2$ (**1a**), monoclinic $P2_1/n$, $a = 10.055(2)$ Å, $b = 35.428(5)$ Å, $c = 15.153(2)$ Å, $\beta = 93.802(3)°$, $V = 5386(1)$ Å^3, $Z = 4$; $[Bu_4N][Cu_3(\mu_3\text{-}OH)(\mu\text{-}pz)_3Cl_3]$ (**1b**), triclinic $P\text{-}1$, $a = 9.135(2)$ Å, $b = 13.631(2)$ Å, $c = 14.510(2)$ Å, $\alpha = 67.393(2)°$, $\beta = 87.979(2)°$, $\gamma = 80.268(3)°$, $V = 1643.2(4)$ Å^3, $Z = 2$; $[PPN]_2[Cu_3(\mu_3\text{-}O)(\mu\text{-}pz)_3Cl_3]$ (**2**), monoclinic $P2/c$, $a = 12.807(2)$ Å, $b = 13.093(2)$ Å, $c = 23.139(4)$ Å, $\beta = 105.391(3)°$, $V = 3741(1)$ Å^3, $Z = 2$; $[PPN]_2[Cu_3(\mu_3\text{-}Cl)_2(\mu\text{-}pz)_3Cl_3]\cdot 0.75H_2O\cdot 0.5CH_2Cl_2$ (**3a**), triclinic $P\text{-}1$, $a = 14.042(2)$ Å, $b = 23.978(4)$ Å, $c = 25.195(4)$ Å, $\alpha = 76.796(3)°$, $\beta = 79.506(3)°$, $\gamma = 77.629(3)°$, $V = 7988(2)$ Å^3, $Z = 4$; $[Bu_4N]_2[Cu_3(\mu_3\text{-}Cl)_2(\mu\text{-}pz)_3Cl_3]$ (**3b**), monoclinic $C2/c$, $a = 17.220(2)$ Å, $b = 15.606(2)$ Å, $c = 20.133(2)$ Å, $\beta = 103.057(2)°$, $V = 5270(1)$ Å^3, $Z = 4$; $[Et_3NH][Cu_3(\mu_3\text{-}OH)(\mu\text{-}pz)_3Cl_3(pzH)]$ (**4**), triclinic $P\text{-}1$, $a = 11.498(2)$ Å, $b = 11.499(2)$ Å, $c = 12.186(2)$ Å, $\alpha = 66.475(3)°$, $\beta = 64.279(3)°$, $\gamma = 80.183(3)°$, $V = 1331.0(5)$ Å^3, $Z = 2$. Magnetic susceptibility measurements show that the three copper centers of **2** are strongly antiferromagnetically coupled with $J_{Cu-Cu} = -500$ cm^{-1}.

Introduction

Polynuclear copper complexes are attracting attention because of their interesting magnetic properties and their relevance to the active centers of a number of metalloproteins.[1,2] With regard to the latter, two recent discoveries add importance to the biological role of polynuclear copper species and provide the impetus for further investigations of complexes containing three or more copper atoms: first, the recognition that the 15 copper atom active center of particulate methane monooxygenase (pMMO) from *Methylococcus capsulatus* (Bath) is organized into two types of five trinuclear aggregates of yet unknown structures[3] and, second, the preliminary structural characterization of nitrous oxide

* To whom correspondence should be addressed. E-mail: (R.G.R.) raphael@adam.uprr.pr.
[+] Present address: Chemistry Department, Texas A&M University, College Station, TX 77843.
[§] University of Puerto Rico.
[‡] Slovak Technical University.
[†] University of Texas at El Paso.
[#] Darmstadt University of Technology.

(1) (a) Ferrer, S.; Haasnoot, J. G.; Reedijk, J.; Müller, E.; Biagini Cigni, M.; Lanfranchi, M.; Manotti Lanfredi, A. M.; Ribas, J. *Inorg. Chem.* **2000**, *39*, 1859 and references therein. (b) Mukherjee, P. S.; Maji, T. K.; Mostafa, G.; Ribas, J.; El Fallah, M. S.; Chaudhuri, N. R. *Inorg. Chem.* **2001**, *40*, 928. (c) Suh, M. P.; Han, M. Y.; Lee, J. H.; Min, K. S.; Hyeon, C. *J. Am. Chem. Soc.* **1998**, *120*, 3819. (d) Kahn, O. *Molecular Magnetism*; VCH: New York, 1993; p 211. (e) Butcher, R. J.; O'Connor, C. J.; Sinn, E. *Inorg. Chem.* **1981**, *20*, 537. (f) Beckett, R.; Colton, R.; Hoskins, B. F.; Martin, R. L.; Vince, D. G. *Aust. J. Chem.* **1969**, *22*, 2527.
(2) (a) Solomon, E. I.; Sundaram, U. M.; Machonkin, T. E. *Chem. Rev.* **1996**, *96*, 2563. (b) da Silva, F. J. J. R; Williams, R. J. P. *The Biological Chemistry of the Elements*; Clarendon Press: 1991; Chapter 15.

10.1021/ic010670l CCC: $22.00
Published on Web 03/26/2002

reductase from *Pseudomonas nautica*-617 which revealed a tetracopper active center containing one capping sulfide and two terminal water/hydroxide ligands.[4]

In this paper we present the synthesis, characterization, and X-ray structure determination of four trinuclear Cu^{II}–pyrazolato complexes—$[Cu_3(\mu_3\text{-OH})(\mu\text{-pz})_3Cl_3]^-$ (as the PPN^+ (**1a**) and Bu_4N^+ (**1b**) salts), $[PPN]_2[Cu_3(\mu_3\text{-O})(\mu\text{-pz})_3Cl_3]$ (**2**), $[Cu_3(\mu_3\text{-Cl})_2(\mu\text{-pz})_3Cl_3]^{2-}$ (as the PPN^+ (**3a**) and Bu_4N^+ (**3b**) salts) and $[Et_3NH][Cu_3(\mu_3\text{-OH})(\mu\text{-pz})_3Cl_3(pzH)]$ (**4**)—along with their chemical interconversions and the magnetic susceptibility study of complex **2**. While trinuclear complexes containing the $Cu_3(\mu_3\text{-OH})(\mu\text{-pz})_3$ moiety with various peripheral ligands have been described before,[5] this is the first report of systematic manipulation of their μ_3-ligands. The characterizations of **2** and **3** provide the first structural reports of the planar $Cu^{II}_3(\mu_3\text{-O})$ and the $Cu^{II}_3(\mu_3\text{-Cl})_2$ motifs.

Experimental Section

All commercially available reagents were used as received, while the solvents were distilled prior to use. Infrared, ^{1}H NMR, and UV–vis spectra were recorded on a Nicolet FT-IR 6000, Bruker ADVANCE DRX-500, and Varian CARY 500 Scan, respectively.

$[PPN][Cu_3(\mu_3\text{-OH})(\mu\text{-pz})_3Cl_3]$ (1a). **1a** is prepared similarly to **1b** (see below) using NaOH and PPNCl. Yield: 65%. Anal. Calcd/Found for **1a**: C, 51.39/51.51; H, 3.71/3.57; N, 9.31/9.25.

$[Bu_4N][Cu_3(\mu_3\text{-OH})(\mu\text{-pz})_3Cl_3]$ (1b). $CuCl_2\cdot 2H_2O$ (1.568 g, 9.20 mmol), pyrazole (626 mg, 9.20 mmol), NaOH (368 mg, 9.20 mmol), and Bu_4NOH (40% aqueous solution) (2.0 mL, 3.06 mmol) are stirred in 23 mL of thf for 16 h at ambient temperature. The initial dark green color of the solution gradually turns deep blue, and a white precipitate is filtered out. To the filtrate is added 70 mL of Et_2O, and the mixture is layered with 40 mL of Et_2O; large blue crystals result after 3 days and are vacuum-dried. Recrystallization from thf/Et_2O affords crystals suitable for X-ray diffraction. Yield: 1.91 g (82%). Mp: 167 °C dec. IR (KBr pellet, 400–1700 cm^{-1}) after subtraction of Bu_4N^+ absorptions: 436 (m), 485 (m), 626 (m), 755 (s), 783 (s), 962 (w), 1052 (vs), 1078 (w), 1157 (w), 1180 (s), 1255 (w), 1278 (m), 1379 (s), 1420 (m), 1430 (m), 1485 (s), 1635 (w). The absorption peaks at 436 and 485 cm^{-1} are tentatively assigned to Cu–O vibrations. UV–vis (CH_2Cl_2, cm^{-1}): 16520. ^{1}H NMR ($CDCl_3$, ppm): 39.07, s (1H, $w_{1/2}$ = 41.4 Hz); 35.93, s (2H, $w_{1/2}$ = 68.5 Hz). Anal. Calcd/Found for **1b**: C, 39.63/39.87; H, 6.13/6.18; N, 12.94/12.86.

$[PPN]_2[Cu_3(\mu_3\text{-O})(\mu\text{-pz})_3Cl_3]$ (2). Method A. To a 35 mL thf solution of NaOH (0.746 g, 18.6 mmol) are added pzH (0.938 g, 13.9 mmol) and $CuCl_2\cdot 2H_2O$ (2.386 g, 13.9 mmol). After the solution is stirred for 15 h at ambient temperature, NaCl is removed by filtration and the volume of the dark green filtrate reduced to ~1/2. Addition of 20 mL of *n*-hexane results in 1.778 g of a dark green solid, which is washed with thf and Et_2O and air-dried. To 327 mg of the dark green solid are added NaOH (24 mg, 0.6 mmol) and PPNCl (681 mg, 1.2 mmol), and the mixture is stirred in 50 mL of thf for 4 h. Complex **2** forms as a brown solid which is filtered out, washed with thf and Et_2O, and vacuum-dried. Yield: 0.831 g (88%).

Method B. $CuCl_2\cdot 2H_2O$ (141 mg, 0.83 mmol), pyrazole (56 mg, 0.83 mmol), NaOH (55 mg, 1.37 mmol), and PPNCl (316 mg, 0.55 mmol) are stirred in 10 mL of CH_2Cl_2 for 12 h at ambient temperature. After filtration, the dark green solution is treated with 50 mL of Et_2O and the resulting solid filtered out and recrystallized by Et_2O diffusion to a CH_2Cl_2 solution. Pure **2** is obtained in ~50% yield after the dark violet crystals are washed with acetone.

Method C. **3a** (103 mg, 0.03 mmol) is dissolved in 2 mL of CH_2Cl_2, and 0.2 mL of a methanolic solution containing NaOH (4.8 mg, 0.12 mmol) is added under stirring. The green color of the solution immediately turns darker. After 5 h, the solution is filtered and Et_2O is diffused into it. Repeating the recrystallization process yields 75 mg (78%) of **2**. Mp: 265 °C dec. Anal. Calcd/Found for **2**: C, 61.08/61.17; H, 4.33/4.59; N, 7.03/7.06; Cl, 6.50/6.65. Complex **2** is an air-stable dark violet crystalline solid which becomes brown-green in powdered samples and in solution. IR (KBr pellet, 400–1700 cm^{-1}) after subtraction of PPN^+ absorptions: 451 (w), 601 (w), 630 (w), 785 (w), 877 (w), 922 (w), 956 (w), 1048 (s), 1194 (w), 1377 (w), 1413 (w). The absorption at 451 cm^{-1} is tentatively assigned to a Cu–O stretching mode. UV–vis (CH_2Cl_2, cm^{-1}): 12500 (sh), 14910. ^{1}H NMR ($CDCl_3$, ppm): 36.95 (1H, $w_{1/2}$ = 53.6 Hz); 36.40 (2H, $w_{1/2}$ = 77.7 Hz). Recrystallization from CH_2Cl_2/Et_2O affords dark violet needles suitable for X-ray diffraction.

$[PPN]_2[Cu_3(\mu_3\text{-Cl})_2(\mu\text{-pz})_3Cl_3]$ (3a). $CuCl_2\cdot 2H_2O$ (426 mg, 2.50 mmol), pyrazole (170 mg, 2.50 mmol), NaOH (100 mg, 2.50 mmol), and PPNCl (957 mg, 1.67 mmol) are stirred in 10 mL of CH_2Cl_2 for 12 h at ambient temperature, and NaCl is filtered out. Treatment of the green filtrate with 50 mL of Et_2O crushes out complex **3a** as a green solid, which is filtered and washed with Et_2O. Yield: 1.35 g (95%). Mp: 204–205 °C. UV–vis (CH_2Cl_2, cm^{-1}): 12500 (sh), 14570. ^{1}H NMR ($CDCl_3$, ppm): 37.29 (1H, $w_{1/2}$ = 50.7 Hz); 36.29 (2H, $w_{1/2}$ = 87.5 Hz). Anal. Calcd/Found for **3a**: C, 57.50/57.90; H, 4.24/4.21; N, 6.58/6.63. Crystals suitable for X-ray diffraction are obtained by vapor diffusion of Et_2O into a CH_2Cl_2 solution of **3a**.

$[Bu_4N]_2[Cu_3(\mu_3\text{-Cl})_2(\mu\text{-pz})_3Cl_3]$ (3b). $CuCl_2\cdot 2H_2O$ (213 mg, 1.25 mmol) is treated as for **3a**, but using TBACl instead of PPNCl. Yield: 420 mg (96%). Mp: 198–199 °C. Anal. Calcd/Found for **3b**: C, 46.70/46.73; H, 7.69/7.88; N, 10.63/10.54; Cl, 16.85/16.59. IR (KBr pellet, 400–1700 cm^{-1}) after subtraction of the Bu_4N^+ absorptions: 628 (w), 960 (w), 1055 (s), 1080 (w), 1151 (w), 1180 (s), 1252 (w), 1274 (w), 1379 (m), 1418 (w), 1433 (w), 1483 (s), 1635 (w, br). UV–vis (CH_2Cl_2, cm^{-1}): 12500 (sh), 14620. ^{1}H NMR ($CDCl_3$, ppm): 39.44 (1H, $w_{1/2}$ = 48.0 Hz); 35.95 (2H, $w_{1/2}$ = 66.0 Hz).

(3) (a) Elliott, S. J.; Randall, D. W.; Britt, R. D.; S. I. Chan *J. Am. Chem. Soc*. **1998**, *120*, 3247. (b) Elliott, S. J.; Zhu, M.; Tso, L.; Nguyen, H.-H. T.; Yip, J. H.-K.; Chan, S. I. *J. Am. Chem. Soc*. **1997**, *119*, 9949. (c) Wilkinson, B.; Zhu, M.; Priestley, N. D.; Nguyen, H.-H. T.; Morimoto, H.; Williams, P. G.; Chan, S. I.; Floss, H. G. *J. Am. Chem. Soc*. **1996**, *118*, 921. (d) Nguyen, H.-H. T.; Nakagawa, K. H.; Hedman, B.; Elliott, S. J.;. Lidstrom, M. E.; Hodgson, K. O.; Chan, S. I. *J. Am. Chem. Soc*. **1996**, *118*, 12766. (e) Nguyen, H.-H. T.; Shiemke, A. K.; Jacobs, S. J.; Hales, B. J.; Lidstrom, M. E.; Chan, S. I. *J. Biol. Chem*. **1994**, *269*, 14995. (f) Chan, S. I.; Nguyen, H.-H. T.; Shiemke, A. K.; Lindstrom, M. E. In *Bioinorganic Chemistry of Copper*; Karlin, K. D., Tyeklar, Z., Eds.; Chapman & Hall: New York, 1993; pp 184–195.

(4) (a) Prudêncio, M.; Pereira, A. S.; Tavares, P.; Besson, S.; Cabrito, I.; Brown, K.; Samyn, B.; Devreese, B.; Van Beeumen, J.; Susnak, F.; Fauque, G.; Moura, J. J. G.; Tegoni, M.; Cambillau, C.; Moura, I. *Biochemistry* **2000**, *39*, 3899. (b) Brown, K.; Tegoni, M.; Prudêncio, M.; Pereira, A. S.; Besson, S.; Moura, J. J.; Moura, I.; Cambillau, M. *Nat. Struct. Biol*. **2000**, *7*, 191. (c) Rasmussen, T.; Berks, B. C.; Sanders-Loehr, J.; Dooley, D. M.; Zumft, W. G.; Thompson, A. J. *Biochemistry* **2000**, *39*, 12753. (d) Alvarez, M. L.; Ai, J.; Zumft, W.; Sanders-Loehr, J.; Dooley, D. M. *J. Am. Chem. Soc*. **2001**, *123*, 576.

(5) (a) Sakai, K.; Yamada, Y.; Tsubomura, T.; Yabuki, M.; Yamaguchi, M. *Inorg. Chem*. **1996**, *35*, 542. (b) Angaroni, M.; Ardizzoia, G. A.; Beringhelli, T.; La Monica, G.; Gatteschi, D.; Masciocchi, N.; Moret, M. *J. Chem. Soc., Dalton Trans*. **1990**, 3305. (c) Hulsbergen, F. B.; ten Hoedt, R. W. M.; Verschoor, G. C.; Reedijk, J.; Spek, A. L. *J. Chem. Soc., Dalton Trans*. **1983**, 539.

Table 1. Crystallographic Data for **1a**, **1b**, **2**, **3a**, **3b**, and **4**

	1a	1b	2	3a	3b	4
empirical formula	$C_{50}H_{50}Cl_5Cu_3N_7O_2P_2$	$C_{25}H_{46}Cl_3Cu_3N_7O$	$C_{81}H_{69}Cl_3Cu_3N_8OP_4$	$C_{81.5}H_{71.5}Cl_6Cu_3N_8O_{0.75}P_4$	$C_{41}H_{81}Cl_5Cu_3N_8$	$C_{18}H_{30}Cl_3Cu_3N_9O$
fw	1210.78	757.66	1591.30	1702.16	1054.01	685.48
temp (K)	298(2)	298(2)	298(2)	298(2)	298(2)	298(2)
wavelength (Å)	0.71073	0.71073	0.71073	0.71073	0.71073	0.71073
cryst syst	monoclinic	triclinic	monoclinic	triclinic	monoclinic	triclinic
space group	$P2_1/n$ (no. 14)	P-1 (no. 2)	$P2/c$ (no.13)	P-1 (no. 2)	$C2/c$ (no. 15)	P-1 (no. 2)
a (Å)	10.055(2)	9.135(2)	12.807(2)	14.042(2)	17.220(2)	11.498(2)
b (Å)	35.428(5)	13.631(2)	13.093(2)	23.978(4)	15.606(2)	11.499(2)
c (Å)	15.153(2)	14.510(2)	23.139(4)	25.195(4)	20.133(2)	12.186(2)
α (deg)	90	67.393(2)	90	76.796(3)	90	66.475(3)
β (deg)	93.802(3)	87.979(2)	105.391(3)	79.506(3)	103.057(2)	64.279(3)
γ (deg)	90	80.268(3)	90	77.629(3)	90	80.183(3)
V (Å^3)	5386.2(13)	1643.2(4)	3740.7(11)	7988(2)	5270.3(10)	1331.0(5)
Z	4	2	2	4	4	2
density(calcd) (Mg m^{-3})	1.493	1.531	1.413	1.415	1.328	1.710
abs coeff (mm^{-1})	1.527	2.198	1.090	1.122	1.488	2.706
F(000)	2468	782	1634	3486	2220	694
cryst size (mm)	0.60 × 0.15 × 0.10	0.30 × 0.28 × 0.16	0.36 × 0.08 × 0.05	0.36 × 0.14 × 0.02	0.18 × 0.14 × 0.12	0.24 × 0.19 × 0.16
no. of independent reflns	7750	4703	5385	22903	3793	3815
R	0.0541	0.0354	0.0315	0.0485	0.0530	0.0468
R_w	0.1111	0.0933	0.0763	0.0820	0.1303	0.1235

Scheme 1

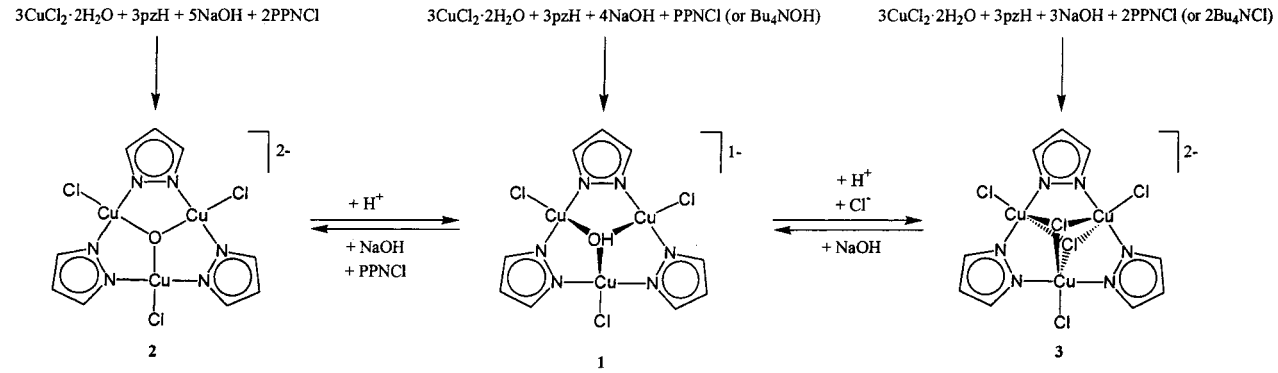

[Et$_3$NH][Cu$_3$(μ_3-OH)(μ-pz)$_3$Cl$_3$(pzH)] (4). From a reaction of $CuCl_2$·$2H_2O$ (170 mg, 1.00 mmol), pzH (68 mg, 1 mmol), and Et_3N (2 mL, 0.5 M/MeOH, 1 mmol) in MeOH, **4** was isolated as a blue crystalline minor product.

X-ray diffraction data, collected from a single crystal mounted atop a glass fiber with a Siemens SMART-CCD diffractometer,[6a] were corrected for Lorentz and polarization effects.[6b] The structures were solved employing the SHELXTL-direct methods program and refined by full-matrix least-squares methods on F^2.[6] Crystallographic details for **1a**, **1b**, **2**, **3a**, **3b**, and **4** are summarized in Table 1.

Determination of the temperature dependence of the magnetic susceptibility for powder sample **2** was conducted by using Faraday-type balances at the applied field of $B = 1.5$ T (sample mass $m =$ 15.945 mg, 97 data points in the temperature range 4.4−290.2 K). In evaluating the molar susceptibility, the molar mass $M_r = 1591.3$ g mol^{-1} has been used. The corrected magnetic susceptibility has been converted to the effective magnetic moment $\mu_{eff}/\mu_B = 798(\chi' T)^{1/2}$ (SI units are employed). A correction for temperature-independent paramagnetism for three copper(II) centers of $\chi_{TIP} = 3 \times 0.75 \times 10^{-9}$ m^3 mol^{-1} has been applied.[7a] The correction for the underlying diamagnetism has been estimated on the basis of Pascal constants: $\chi_{dia}(1) = -11.775 \times 10^{-9}$ m^3 mol^{-1}.[7b] When the measured magnetic susceptibility of the triphenylphosphine unit is used ($\chi(PPh_3) = -2.021 \times 10^{-9}$ m^3 mol^{-1}),[8] a slightly reduced value results: $\chi_{dia}(2) = -10.681 \times 10^{-9}$ m^3 mol^{-1}.

Results

Complexes **1**−**3** are all prepared from equimolar mixtures of $CuCl_2$ and pzH, the differentiation among them being determined by the amounts of available NaOH, chloride, and counterions (Scheme 1). Their μ_3-ligand exchange reactions are followed in solution by UV−vis spectroscopy monitoring the growth or disappearance of the respective absorption peaks. The identity of the transformation products is then confirmed in each case by infrared spectroscopy and by comparison of the unit cell dimensions of the isolated crystalline solid with those of the X-ray structures of **1**−**3**. Species **1** and **2**, which differ by one H^+ but have quite different solubility properties, are in a pH-, counterion-, and solvent-dependent equilibrium in solution. The μ_3-OH species **1** forms in the presence of 4 equiv of hydroxide per trinuclear unit, while an additional 1 equiv of hydroxide is required for the synthesis of the μ_3-O species **2**. In solvents where both **1** and **2** are well soluble (i.e., CH_2Cl_2), the equilibrium between them is controlled by pH. However, in solvents

(6) (a) *Data Collection: SMART-NT Software Reference Manual*, version 5.0; Bruker AXS, Inc.: Madison, WI, 1998. (b) *Data Reduction: SAINT-NT Software Reference Manual*, verion 4.0; Bruker AXS, Inc.: Madison, WI, 1996. (c) Sheldrick, G. M. *SHELXTL-NT*, version 5.1; Bruker AXS, Inc.: Madison, WI, 1999.

(7) (a) Weiss, A.; Witte, H. *Magnetochemie*; Verlag Chemie: Weinheim, Germany, 1973. (b) König, E. *Landolt-Börnstein, Neue Serie*; Springer: Berlin, 1966; Vol. II/2, pp 1−16.

(8) Gupta, R. G. *Landolt-Börnstein, Neue Serie*; Springer: Berlin, 1986; Vol. II/16.

Scheme 2

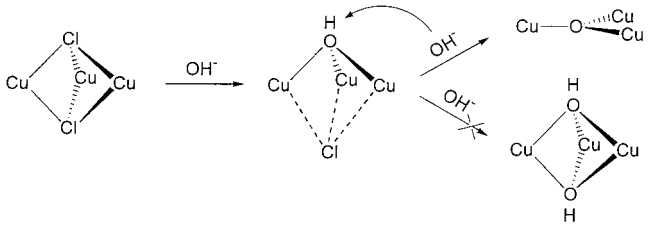

where their solubilities are significantly different, the equilibrium is influenced by the nature and concentration of the counterion, as well. For example, addition of PPN^+ to thf solutions of **1a** or **1b** shifts the equilibrium toward the thf-insoluble complex **2**, as the latter slowly precipitates out of solution as a PPN^+ salt. In contrast, with Bu_4N^+ as counterion, the μ_3-O species **2** does not precipitate easily, nor crystallize, and Bu_4N^+ does not influence the equilibrium of **1** and **2**. Complex **2** is insoluble in dry thf, but readily dissolves in wet thf as it becomes protonated, converting to **1**.

While stoichiometric addition of 1 equiv of PPN^+ to **1a** in thf leads to precipitatation of **2**, an excess of PPNCl initiates the conversion of **1** to **3** by virtue of the increased Cl^- concentration. The equilibrium between **1** and **3** is pH- and chloride-concentration-dependent. Controlled acidification of solutions of **1** protonates the μ_3-OH, eliminating H_2O from the trimer, as the μ_3-position becomes occupied by Cl. Further addition of HCl to **3** leads to destruction of the trimeric ring with formation of $CuCl_4^{2-}$ and pzH. However, in the absence of acids, the $Cu_3(\mu\text{-pz})_3Cl_3$ frame remains intact during the above transformations, which only exchange the μ_3-species.

Reaction of the $Cu_3(\mu_3\text{-Cl})_2$ complex **3** with NaOH reforms the μ_3-OH bridge by replacing one μ_3-Cl. A possible intermediate species between **3** and **1**, containing both a μ_3-OH and a loosely held μ-Cl (Scheme 2), may be an analogue of complex **4**. The latter has been found in a reaction mixture involving $CuCl_2$/pzH/base in a 1:1:1 ratio, conditions appropriate for an intermediate between **1** and **3**. A species similar to **4** has also been found in the structure of a related tricopper−pyrazolato complex.[5b] Further addition of OH^- does not lead to formation of a $Cu_3(\mu_3\text{-OH})_2$ species, but to deprotonation of the bridging hydroxide, producing the oxo complex **2**. As a result of the equilibria described in the preceding paragraphs, complexes **1**−**3** can all three transiently coexist under the appropriate conditions in nonequilibrium solutions. Yet, analytically pure crystalline solid samples can be obtained from such solutions, taking advantage of the distinct solubility of each complex.

Complexes **1** and **2** are ESR-silent at ambient as well as at liquid nitrogen temperature, probably due to a fast electron spin relaxation, as has been previously observed for related complexes.[5c,9] As expected, all three complexes **1**−**3** show paramagnetically shifted resonances in their ^1H NMR spectra: the presence of two resonances—one for the protons at the 3- and 5-pz positions and one for the proton at the 4-pz position—for each complex shows the magnetic equivalence of the three pyrazole rings in solution.

(9) Complex **3** has well-resolved ESR spectra at 300 and 77 K, which will be discussed elsewhere along with the analysis of its magnetic susceptibility measurements.

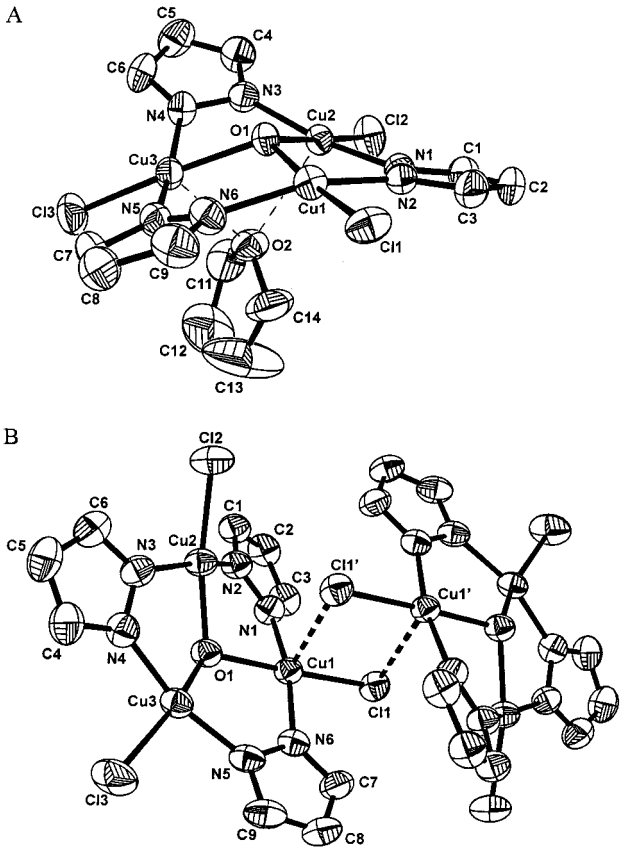

Figure 1. ORTEP drawing for compounds **1a** (A) and **1b** (B) showing the atom labeling scheme. Thermal ellipsoids at the 50% probability level. Hydrogen atoms omitted.

X-ray Structures. All four complexes **1**−**4** consist of a nine-membered $[Cu-N-N]_3$ metallacycle where each Cu atom is also coordinated to a terminal chlorine atom (or two chlorines and one pyrazole for **4**). The center of this metallacycle accommodates triply bridging hydroxide, oxide, or chloride ligands, respectively, with accompanying changes to the complex-anion geometry. In their crystalline form, complexes **1a** and **1b** (Figure 1) contain a pyramidal μ_3-OH group bridging unsymmetrically the three Cu atoms—the Cu−OH bond lengths range from 1.987(3) to 2.035(3) Å and Cu−O−Cu angles between 104.4(1)° and 118.5(2)° while the three chlorine atoms are on the opposite side of their *trans*-μ_3-OH, with respect to the metallacycle. The O atom is 0.524 and 0.506 Å out of the Cu_3 plane for **1a** and **1b**, respectively. The Cu···Cu intramolecular distances are within the 3.206(1)−3.447(1) Å range, while the shortest corresponding intermolecular Cu(1)···Cu(1′) distances are 3.618(1) Å for **1a** and 3.430(1) Å for **1b,** resulting from weak interactions between the copper and chlorine atoms of adjacent trimers. All Cu atoms are in a distorted square-planar geometry with *trans* O−Cu−Cl and N−Cu−N angles in the ranges of 160.02(8)−177.22(10)° and 160.0(2)−169.0(1)°, respectively. The best-fit planes of the pyrazole rings form dihedral angles of 4.5−34.5° with the Cu_3 plane. The PPN cations of **1a** generate large voids in the crystalline

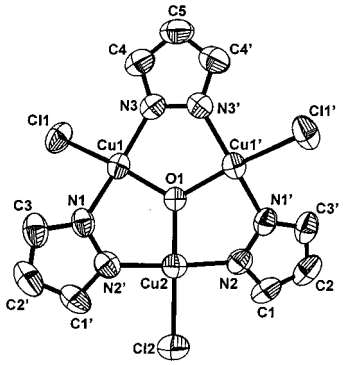

Figure 2. ORTEP drawing for compound **2** showing the atom labeling scheme. Thermal ellipsoids at the 50% probability level. Hydrogen atoms omitted.

Table 2. Selected Bond Lengths (Å) and Angles (deg) for **1a**

Cu(1)···Cu(2)	3.447(1)	Cu(1)−O(1)−Cu(2)	118.54(15)
Cu(1)···Cu(3)	3.434(1)	Cu(1)−O(1)−Cu(3)	117.26(15)
Cu(2)···Cu(3)	3.206(1)	Cu(2)−O(1)−Cu(3)	104.38(13)
Cu(1)−O(1)	1.987(3)	O(1)−Cu(1)−Cl(1)	172.91(10)
Cu(2)−O(1)	2.024(3)	O(1)−Cu(2)−Cl(2)	177.22(10)
Cu(3)−O(1)	2.035(3)	O(1)−Cu(3)−Cl(3)	175.34(10)
Cu(1)−Cl(1)	2.313(1)	N(6)−Cu(1)−N(1)	159.98(17)
Cu(2)−Cl(2)	2.261(1)	N(3)−Cu(2)−N(2)	167.33(17)
Cu(3)−Cl(3)	2.263(2)	N(5)−Cu(3)−N(4)	163.48(17)
Cu(1)−N(1)	1.951(4)	N(2)−N(1)−Cu(1)	121.0(3)
Cu(1)−N(6)	1.953(4)	N(1)−N(2)−Cu(2)	122.3(3)
Cu(2)−N(3)	1.940(4)	N(4)−N(3)−Cu(2)	118.8(3)
Cu(2)−N(2)	1.953(4)	N(3)−N(4)−Cu(3)	118.2(3)
Cu(3)−N(5)	1.940(4)	N(6)−N(5)−Cu(3)	122.1(3)
Cu(3)−N(4)	1.946(4)	N(5)−N(6)−Cu(1)	121.1(3)

Table 3. Selected Bond Lengths (Å) and Angles (deg) for **1b**

Cu(1)···Cu(2)	3.247(1)	Cu(1)−O(1)−Cu(2)	107.34(11)
Cu(1)···Cu(3)	3.431(1)	Cu(1)−O(1)−Cu(3)	117.98(12)
Cu(2)···Cu(3)	3.401(1)	Cu(2)−O(1)−Cu(3)	116.16(12)
Cu(1)−O(1)	2.014(2)	O(1)−Cu(1)−Cl(1)	177.08(7)
Cu(2)−O(1)	2.018(2)	O(1)−Cu(2)−Cl(2)	169.07(8)
Cu(3)−O(1)	1.989(2)	O(1)−Cu(3)−Cl(3)	160.02(8)
Cu(1)−Cl(1)	2.315(1)	N(6)−Cu(1)−N(1)	169.03(13)
Cu(2)−Cl(2)	2.255(1)	N(3)−Cu(2)−N(2)	160.47(13)
Cu(3)−Cl(3)	2.252(1)	N(5)−Cu(3)−N(4)	164.57(13)
Cu(1)−N(1)	1.952(3)	N(2)−N(1)−Cu(1)	117.7(2)
Cu(1)−N(6)	1.943(3)	N(1)−N(2)−Cu(2)	120.0(2)
Cu(2)−N(3)	1.937(3)	N(4)−N(3)−Cu(2)	121.6(2)
Cu(2)−N(2)	1.939(3)	N(3)−N(4)−Cu(3)	120.9(2)
Cu(3)−N(5)	1.932(3)	N(6)−N(5)−Cu(3)	122.8(2)
Cu(3)−N(4)	1.952(3)	N(5)−N(6)−Cu(1)	121.1(2)

lattice, which are filled by solvent molecules—one CH_2Cl_2 and one thf molecule per trimer. The interstitial thf molecule is positioned with its O atom directed toward two of the trimer Cu atoms, with long Cu···O interactions of 2.495(4) and 2.550(4) Å, which do not cause any significant distortion of its geometry compared to that of **1b**. Tables 2 and 3 list important bond lengths and angles for **1a** and **1b**, respectively.

The dianionic complex **2** consists of a planar $Cu_3(\mu_3\text{-O})$ core supported by bridging pyrazolates, while terminal chloride ligands complete the approximate square-planar coordination of the Cu atoms (Figure 2). A crystallographic 2-fold axis, running through Cu(2), O(1), and C(5), bisects complex **2**, yet the $[Cu_3(\mu_3\text{-O})(\mu\text{-pz})_3Cl_3]^{2-}$ ion has approximate 3-fold symmetry: The $Cu_3(\mu_3\text{-O})$ moiety is approximately trigonal planar with an average Cu−O distance and Cu−O−Cu angle of 1.891(2) Å and 120.0(1)°,

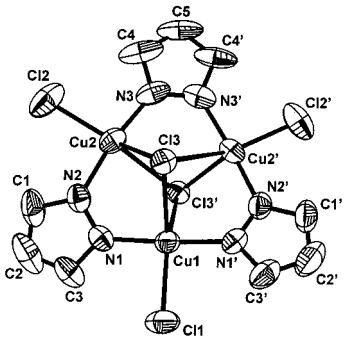

Figure 3. ORTEP drawing for compound **3b** showing the atom labeling scheme. Thermal ellipsoids at the 30% probability level. Hydrogen atoms omitted.

Table 4. Selected Bond Lengths (Å) and Angles (deg) for **2**

Cu(1)···Cu(2)	3.269(1)	Cu(1)−O(1)−Cu(2)	119.59(8)
Cu(1)···Cu(1′)	3.287(1)	Cu(1′)−O(1)−Cu(1)	120.82(15)
Cu(1′)···Cu(2)	3.269(1)	O(1)−Cu(1)−Cl(1)	158.99(4)
Cu(1)−O(1)	1.890(2)	O(1)−Cu(2)−Cl(2)	180.0
Cu(2)−O(1)	1.893(3)	N(3)−Cu(1)−N(1)	158.66(11)
Cu(1)−Cl(1)	2.295(1)	N(2)−Cu(2)−N(2′)	175.46(18)
Cu(2)−Cl(2)	2.298(2)		
Cu(1)−N(1)	1.958(3)		
Cu(1)−N(3)	1.946(3)		
Cu(2)−N(2)	1.951(3)		

respectively. This arrangement holds the Cu atoms at average distances of 3.273(1) Å. The short Cu−O bonds pull the $[Cu(\mu\text{-pz})]_3$ frame inward forcing one pyrazole to rotate out of the Cu_3O plane, while the other two pyrazoles are bent by 33.0° out and on either side of this plane. Similarly to **1a** and **1b**, the Cu atoms of **2** deviate from ideal square-planar coordination with O−Cu−Cl angles of 158.99(4)° and 180.0° and N−Cu−N angles of 158.7(1)° and 175.5(2)°. There are no short intermolecular contacts in the solid state. Table 4 lists important bond lengths and angles for **2**.

The crystal structure of complex **3a** shows two independent trimers per asymmetric unit, while that of **3b** shows the trimer bisected by a 2-fold axis (Figure 3). In both structures, the copper and terminal chloride atoms are in an approximately planar arrangement. Two additional chlorides cap unsymmetrically the trimer on either side at distances of 1.674−1.716 Å from the Cu_3 plane, completing the distorted trigonal-bipyramidal coordination of Cu atoms. The $(\mu_3\text{-Cl})$−Cu distances range between 2.341(2) and 3.056(2) Å without a consistent short/long pattern; each μ_3-Cl atom shows one short/two long, two short/one long, or one short/one intermediate/one long Cl−Cu distances. In the absence of a μ_3-OH or μ_3-O, which bind strongly to all three metal atoms, the Cu atoms of **3** are further apart from each other than in **1** or **2**; Cu···Cu distances vary between 3.375(1) and 3.546(1) Å. The pyrazole rings form dihedral angles of 3.7−25.9° with the Cu_3 plane. Tables 5 and 6 list important bond lengths and angles for **3a** and **3b**, respectively.

Comparison of the structure of **4** (Figure 4) with those of **1a,b** shows that the $[Cu-N-N]_3$ ring as well as the $Cu_3(\mu_3\text{-OH})$ fragment is, within experimental error, identical in all three complex anions. Two of the Cu atoms are four-coordinate distorted square-planar, while the third one shows 4 + 1 coordination with a terminal pyrazole completing the square basal plane and a long interaction with a chloride

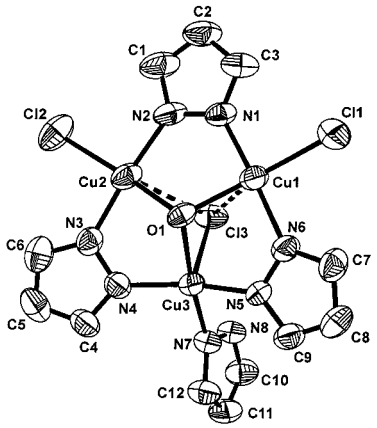

Figure 4. ORTEP drawing for compound **4** showing the atom labeling scheme. Thermal ellipsoids at the 50% probability level. Hydrogen atoms omitted.

Table 5. Selected Bond Lengths (Å) and Angles (deg) for **3a**

Cu(1)···Cu(2)	3.486(1)	Cu(3)−Cl(7)−Cu(1)	86.75(5)
Cu(1)···Cu(3)	3.375(1)	Cu(2)−Cl(8)−Cu(3)	84.94(5)
Cu(2)···Cu(3)	3.455(1)	Cu(2)−Cl(8)−Cu(1)	85.89(5)
Cu(4)···Cu(5)	3.410(1)	Cu(3)−Cl(8)−Cu(1)	75.51(4)
Cu(4)···Cu(6)	3.395(1)	Cu(5)−Cl(9)−Cu(4)	85.97(5)
Cu(5)···Cu(6)	3.494(1)	Cu(6)−Cl(10)−Cu(4)	88.05(6)
Cu(1)−Cl(1)	2.307(2)	Cl(1)−Cu(1)−Cl(7)	135.92(7)
Cu(2)−Cl(2)	2.244(2)	Cl(1)−Cu(1)−Cl(8)	139.91(6)
Cu(3)−Cl(3)	2.282(2)	Cl(7)−Cu(1)−Cl(8)	84.16(5)
Cu(1)−Cl(7)	2.461(2)	Cl(2)−Cu(2)−Cl(8)	138.41(9)
Cu(1)−Cl(8)	2.756(2)	Cl(3)−Cu(3)−Cl(7)	133.65(6)
Cu(2)−Cl(8)	2.341(2)	Cl(3)−Cu(3)−Cl(8)	141.99(6)
Cu(3)−Cl(7)	2.453(2)	Cl(7)−Cu(3)−Cl(8)	84.31(5)
Cu(3)−Cl(8)	2.756(2)	Cl(4)−Cu(4)−Cl(10)	140.64(8)
Cu(4)−Cl(4)	2.265(2)	Cl(4)−Cu(4)−Cl(9)	131.98(7)
Cu(4)−Cl(10)	2.486(2)	Cl(10)−Cu(4)−Cl(9)	87.37(6)
Cu(4)−Cl(9)	2.641(2)	Cl(5)−Cu(5)−Cl(9)	132.52(7)
Cu(5)−Cl(5)	2.262(2)	Cl(6)−Cu(6)−Cl(10)	143.57(10)
Cu(5)−Cl(9)	2.350(2)	N(6)−Cu(1)−N(1)	169.8(2)
Cu(6)−Cl(6)	2.269(2)	N(3)−Cu(2)−N(2)	161.1(2)
Cu(6)−Cl(10)	2.398(2)	N(5)−Cu(3)−N(4)	169.16(19)
Cu(1)−N(1)	1.937(5)	N(7)−Cu(4)−N(12)	174.1(2)
Cu(1)−N(6)	1.929(5)	N(8)−Cu(5)−N(9)	159.7(2)
Cu(2)−N(3)	1.945(5)	N(11)−Cu(6)−N(10)	167.2(2)
Cu(2)−N(2)	1.946(5)	N(2)−N(1)−Cu(1)	123.3(4)
Cu(3)−N(5)	1.931(5)	N(1)−N(2)−Cu(2)	123.1(4)
Cu(3)−N(4)	1.938(5)	N(4)−N(3)−Cu(2)	122.0(4)
Cu(4)−N(7)	1.940(5)	N(6)−N(5)−Cu(3)	122.2(4)
Cu(4)−N(12)	1.947(5)	N(5)−N(6)−Cu(1)	120.7(4)
Cu(5)−N(8)	1.925(5)	N(8)−N(7)−Cu(4)	121.9(4)
Cu(5)−N(9)	1.926(5)	N(7)−N(8)−Cu(5)	121.7(4)
Cu(6)−N(11)	1.930(5)	N(10)−N(9)−Cu(5)	122.7(4)
Cu(6)−N(10)	1.936(5)	N(9)−N(10)−Cu(6)	124.1(4)
		N(12)−N(11)−Cu(6)	121.5(4)
		N(11)−N(12)−Cu(4)	121.7(4)
		N(3)−N(4)−Cu(3)	123.0(4)

Table 6. Selected Bond Lengths (Å) and Angles (deg) for **3b**

Cu(1)···Cu(2)	3.387(1)	Cu(2)−Cl(3)−Cu(1)	86.05(5)
Cu(2)···Cu(2′)	3.546(1)	Cl(1)−Cu(1)−Cl(3)	137.11(3)
Cu(1)−Cl(1)	2.291(2)	Cl(3)−Cu(1)−Cl(3′)	85.77(7)
Cu(2)−Cl(2)	2.265(2)	Cl(2)−Cu(2)−Cl(3)	135.27(8)
Cu(1)−Cl(3)	2.600(2)	N(1)−Cu(1)−N(1′)	176.2(3)
Cu(2)−Cl(3)	2.357(2)	N(2)−Cu(2)−N(3)	163.4(2)
Cu(1)−N(1)	1.927(5)	N(2)−N(1)−Cu(1)	122.1(4)
Cu(2)−N(3)	1.932(5)	N(1)−N(2)−Cu(2)	121.5(4)
Cu(2)−N(2)	1.934(5)	N(3)−N(3′)−Cu(2)	124.0(2)

ion at the apical position of a square pyramid. The latter occupies the unsymmetrically triply bridging position opposite to μ_3-OH with respect to the Cu_3 plane. As one side of the Cu_3 plane is capped by the strongly coordinating μ_3-OH ligand, only weak interactions exist between the three Cu atoms and the chloride ion capping its opposite side—

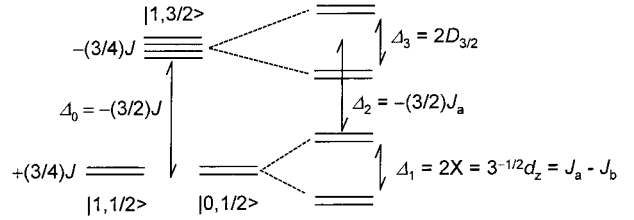

Figure 5. Magnetic energy levels upon involvement of individual exchange interactions: Δ_0, splitting by isotropic exchange for an equilateral triangle (D_{3h} group); Δ_3, zero-field splitting by asymmetric exchange; Δ_1, splitting by the Jahn−Teller effect (E−e vibronic coupling within the D_{3h} group), antisymmetric exchange, or isotropic exchange for an isosceles triangle (C_{2v} group).

Table 7. Selected Bond Lengths (Å) and Angles (deg) for **4**

Cu(1)···Cu(2)	3.414(2)	Cu(1)−O(1)−Cu(2)	116.35(19)
Cu(1)···Cu(3)	3.277(2)	Cu(1)−O(1)−Cu(3)	108.90(18)
Cu(2)···Cu(3)	3.254(2)	Cu(2)−O(1)−Cu(3)	107.99(18)
Cu(1)−Cl(1)	2.257(2)	Cu(1)−Cl(3)−Cu(2)	63.36(4)
Cu(2)−Cl(2)	2.316(2)	Cu(1)−Cl(3)−Cu(3)	64.37(4)
Cu(3)−Cl(3)	2.676(2)	Cu(2)−Cl(3)−Cu(3)	67.93(4)
Cu(1)···Cl(3)	3.375(2)	Cl(1)−Cu(1)−O(1)	169.16(14)
Cu(2)···Cl(3)	3.111(2)	Cl(2)−Cu(2)−O(1)	167.57(13)
Cu(1)−O(1)	2.012(4)	N(7)−Cu(3)−O(1)	170.90(19)
Cu(2)−O(1)	2.006(4)	Cl(1)−Cu(1)−Cl(3)	128.90(9)
Cu(3)−O(1)	2.016(4)	Cl(2)−Cu(2)−Cl(3)	124.28(7)
Cu(1)−N(1)	1.929(5)	N(7)−Cu(3)−Cl(3)	93.09(16)
Cu(1)−N(6)	1.945(5)	N(1)−Cu(1)−N(6)	172.5(2)
Cu(2)−N(2)	1.949(5)	N(2)−Cu(2)−N(3)	174.4(2)
Cu(2)−N(3)	1.932(5)	N(4)−Cu(3)−N(5)	160.0(2)
Cu(3)−N(4)	1.950(5)	N(2)−N(1)−Cu(1)	122.0(4)
Cu(3)−N(5)	1.937(5)	N(5)−N(6)−Cu(1)	119.2(4)
Cu(3)−N(7)	2.016(5)	N(1)−N(2)−Cu(2)	122.4(4)
		N(4)−N(3)−Cu(2)	118.9(4)
		N(3)−N(4)−Cu(3)	118.8(4)
		N(6)−N(5)−Cu(3)	119.3(3)

Cu−Cl = 2.676(2), 3.111(2), and 3.375(2) Å (Table 7)—longer than the corresponding distances in the $Cu_3(\mu_3\text{-Cl})_2$ complexes **3**.

Magnetic Data Analysis. The exchange coupling of three $S_1 = S_2 = S_3 = 1/2$ centers results in eight magnetic states $|S_{12},S\rangle$: two doublets, $|0, 1/2\rangle$ and $|1, 1/2\rangle$, and a quartet, $|1, 3/2\rangle$.[10,11] Here S_{12} is the intermediate spin ($|S_1 - S_2| \le S_{12} \le S_1 + S_2$) and S is the final spin on the addition of spin angular momenta. Their relative energy depends on the topology of the interacting centers and type of interaction involved (Figure 5).

(1) For the isotropic exchange when the interacting centers form an equilateral triangle (D_{3h} point group), the two doublets are degenerate; for the antiferromagnetic interaction ($J < 0$) these are apparently the ground state ^{2}E, whereas for the ferromagnetic exchange ($J > 0$) the quartet ^{4}A is the ground state. The simple isotropic exchange Hamiltonian of the form

$$\hat{H}^{\text{iso}} = -J(\vec{S}_1\cdot\vec{S}_2 + \vec{S}_1\cdot\vec{S}_3 + \vec{S}_2\cdot\vec{S}_3)\hbar^{-2} \qquad (1)$$

yields the analytic formula for the mean magnetic susceptibility (evaluated via the van Vleck equation)

$$\bar{\chi}_{\text{mol}} = C_0\frac{g_{\text{Cu}}{}^2}{4T}\frac{1 + 5\exp[(3/2)J/kT]}{1 + \exp[(3/2)J/kT]} \qquad (2)$$

(10) Kahn, O. *Molecular Magnetism*; VCH Publishers: New York, 1993.

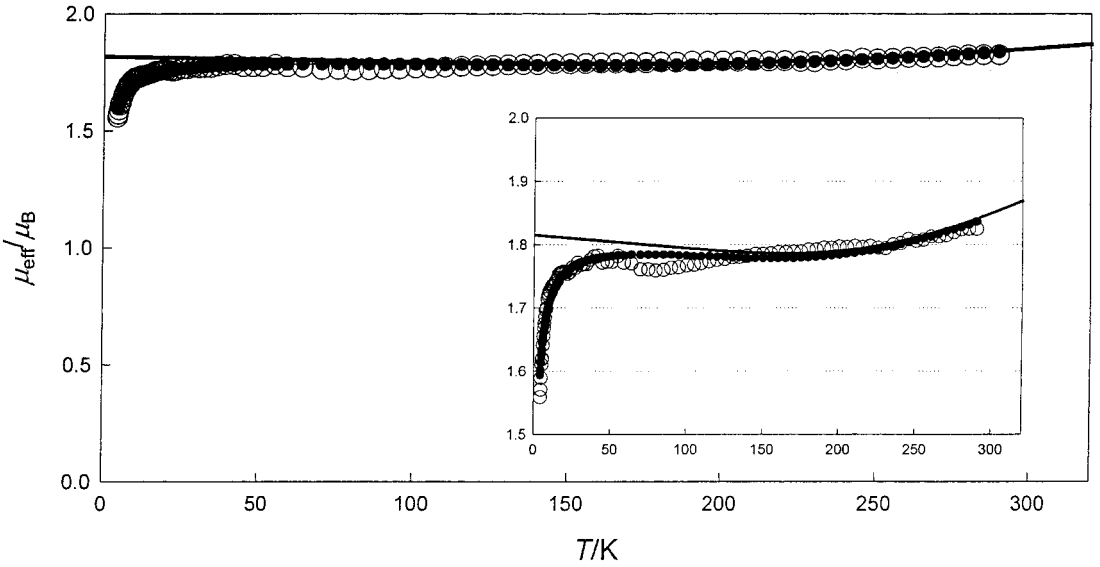

Figure 6. Temperature dependence of the effective magnetic moment for **2**: open circles, experimental data; filled circles, the best-fit values; full line, absence of a molecular field correction.

where $C_0 = N_A\mu_0\mu_B{}^2/k$ comprises the fundamental physical constants in their usual meanings.

(2) The actual crystal packing may induce lower than D_{3h} symmetry. For the geometry of an isosceles triangle (C_{2v} point group; two coupling constants are involved), the isotropic exchange causes a splitting of the doublet states. The isotropic exchange Hamiltonian

$$\hat{H}^{iso} = \hbar^{-2}[-J_a(\vec{S}_1\cdot\vec{S}_2 + \vec{S}_1\cdot\vec{S}_3) - J_b(\vec{S}_2\cdot\vec{S}_3)] \qquad (3)$$

then yields

$$\bar{\chi}_{mol} = [C_0 g_{Cu}{}^2/(4T)]\{10\exp[-(\Delta_1 + \Delta_2)/kT] + \exp(-\Delta_1/kT) + 1\}/\{2\exp[-(\Delta_1 + \Delta_2)/kT] + \exp(-\Delta_1/kT) + 1\} \quad (4)$$

with $\Delta_1 = J_a - J_b$ and $\Delta_2 = -(3/2)J_a$.

(3) The Jahn−Teller effect excludes an orbitally degenerate ground state: there exists an internal disposition of the complex for a geometrical distortion that removes the orbital degeneracy. For the D_{3h} system the distortion applies along the e-mode, resulting in distortion of the equilateral triangle to form an isosceles one. Owing to the E−e vibronic coupling for the D_{3h} group, the magnetic energy levels become $E_-(S = 1/2) = -(1/2)X$ and $E_+(S = 1/2) = +(3/2)X$, where the vibronic coupling parameter $X = V_e{}^2/F_{ee}$ is introduced through the ratio of the vibronic (electron−nuclear) coupling constant (V_e) and the force constant (F_{ee}) calculated along the e-mode of the nuclear displacement (Q_e). Consequently

$$\bar{\chi}_{mol} = [C_0 g_{Cu}{}^2/(4T)]\{10\exp[(3/2)J/kT] + \exp[(1/2)X/kT] + \exp[-(3/2)X/kT]\}/\{2\exp[(3/2)J/kT] + \exp[(1/2)X/kT] + \exp[-(3/2)X/kT]\} \quad (5)$$

For $X = 0$ this relaxes to the usual formula for an equilateral triangle ($\Delta_1 = 0$).

(4) The exchange interaction is not restricted to the case of the isotropic exchange alone. The Cartesian spin−spin interaction tensor can be decomposed into its irreducible components and the spin Hamiltonian rewritten as a sum of the isotropic exchange, the antisymmetric exchange, and the asymmetric exchange contributions.[11,12] Omitting the details, the net effect of the asymmetric exchange for the $S_1 = S_2 = S_3 = 1/2$ system is the zero-field splitting of the quartet state $|1, 3/2\rangle$ into two Kramers doublets (Figure 5). The antisymmetric exchange, on the contrary, results in the removal of the degeneracy for the two doublets $|0, 1/2\rangle$ and $|1, 1/2\rangle$, yielding $E_\pm = (3/4)J \pm d_z/(2\sqrt{3})$.

In summary, the orbitally degenerate ground state, ^{2}E, of the equilateral triangulo complex can be further split into two Kramers doublets, owing to either the geometrically evident departure toward the lower (C_{2v}) symmetry by the Jahn−Teller effect[13] or the antisymmetric exchange.

The magnetic susceptibility of **2** increases upon cooling. The temperature dependence of the effective magnetic moment for **2** is shown in Figure 6. It can be seen that, upon temperature lowering, the effective magnetic moment per formula unit slightly decreases until 70 K and lies around $\mu_{eff} = 1.8\ \mu_B$. This is an indication of the strong antiferromagnetic exchange owing to which only the lowest doublets are populated at temperatures below ambient. On further cooling, a local maximum is identified at 50 K on the μ_{eff} vs T curve (a similar behavior has been reported for another triangulo copper−pyrazolato complex[5b]). Below 30 K a pronounced drop of the effective magnetic moment exists.

The fitting of the magnetic data was performed using the above-mentioned methods, in which the theoretical molar magnetic susceptibility was further corrected for the molecular field, Z, and the temperature-independent term, α, as follows:

$$\chi_{mol}^{calcd} = \frac{\chi^{theor}}{1 - Z\chi^{theor}} + \alpha \qquad (6)$$

(11) Boča, R. *Theoretical Foundations of Molecular Magnetism*; Elsevier: Amsterdam, 1999.

The molecular field correction in the form $Z = N_A\mu_0\mu_B{}^2(zJ')g^2 = N_A\mu_0\mu_B{}^2Y$ involves the term $Y = (zJ')g^2$; J' is the effective intermolecular coupling constant and z the number of neighbors. The full list of free parameters for the optimization is the local magnetogyric ratio, g_{Cu}, the isotropic exchange constant, J_{Cu-Cu}, the molecular field parameter, Y, and the temperature-independent correction, α. A sophisticated nonlinear optimization ("simulated annealing" method combined with a genetic algorithm) has been applied and repeated several times to localize the global minimum rather than the local minima of the error functional.[14,15]

The best results of the fitting are displayed in Figure 6 along with the experimental data. The final set of magnetic parameters based on function 2 is $J_{Cu-Cu} = -500$ cm^{-1}, $g_{Cu} = 2.10$, $Y = -0.82$ cm^{-1}, and $\alpha = -1.17 \times 10^{-9}$ m^3 mol^{-1} (the discrepancy factor $R(\chi) = 0.022$). The very negative coupling constant J_{Cu-Cu} -500 cm^{-1} confirms the existence of a strong antiferromagnetic exchange within the cluster. This feature is quite typical for pyrazolate-bridged Cu atoms.[5b] Such a high value, however, cannot be determined accurately on the basis of the magnetic data limited to 300 K. The value of the isotropic magnetogyric ratio, $g_{Cu} = 2.10$, lies slightly below the usual range owing to the square-planar arrangement of the copper(II) ions. Only a slight correction to the temperature-independent susceptibility, $\alpha = -1.17 \times 10^{-9}$ m^3 mol^{-1}, has been found (this influences the high-temperature data), showing that the overall correction ($\chi_{TIP} + \chi_{dia}$) should be more negative. Probably the TIP contribution was overestimated for the square-planar copper(II) arrangement. Application of a molecular field correction is necessary, as its absence results in a plateau of the μ_{eff} vs T curve (solid line in Figure 6).

The vibronic coupling parameter X, eq 5, is rather insensitive to alteration, and its accuracy is again limited. This is due to the fact that the effect of X superimposes that of the molecular field correction (Z or Y). Attempts to determine the axial zero-field splitting parameter due to the asymmetric exchange, $D_{3/2}$, failed owing to nearly equal population of the two Kramers doublets $|1, 3/2, M_S = \pm 1/2\rangle$ and $|1, 3/2, M_S = \pm 3/2\rangle$ above ambient temperature. The model of an isosceles triangle with two coupling constants did not provide a better fit. Inclusion of a paramagnetic impurity ($S = 1/2$) correction has no significant effect, since it is the same as that for the triangulo copper(II) compound with an $S = 1/2$ ground state.

Discussion

When linear two-coordinate or *trans*-square-planar metal centers are employed, the 60° orientation of the pyrazole N-donor orbitals favors the formation of trimeric metallocycles.[16] While a few examples of nuclearities other than trimeric do exist in binary metal−pyrazolato complex chemistry,[17] trimeric species are the most common. This implies some preference for the $[M-N-N]_3$ metallacycle geometry, which becomes apparent in the course of the chemistry described here. The trimeric $[Cu^{II}(\mu\text{-pz})Cl]_3$ frame is assembled in one step and remains intact when treated with a variety of reagents, including bases and dilute acids. The trimeric copper−pyrazolate metallacycle generates a void in its center, which is filled by μ_3-ligands. To accommodate the geometrical requirements of the pyramidal μ_3-OH and μ_3-Cl, or the planar μ_3-O ligands, the $[Cu-N-N]_3$ ring distorts accordingly by bending to a small extent the N−Cu−N and Cu−N−N angles, or by bending and rotating the pyrazole planes out of the best-fit plane of the metallacyclic ring, without, however, significant changes to the Cu−N and N−N bond lengths. This "breathing" of the metallacycle is reflected in the intramolecular Cu···Cu distances, which vary from an average of 3.273 Å for the μ_3-O complex **2** with short Cu−O bonds, through the 3.361 Å distance of complexes **1** containing a μ_3-OH bridge, to the longer 3.437 Å distance of **3**, the latter forced by the longer Cu−(μ_3-Cl) bonds.

The $[Cu^{II}(\mu\text{-pz})]_3$ metallacycle provides the frame on which H_2O is deprotonated twice, forming μ_3-OH and μ_3-O species in consecutive steps. Complexes containing the $Cu_3(\mu_3\text{-OH})$ moiety have been reported with pyrazolate,[5] triazolate,[18] carboxylate,[19] hexaaza macrocyclic,[20] diphosphinomethane (a Cu^I complex),[21] and aminooximato[1e,22] bridging ligands forming the metallacycle. Of those, the macrocyclic system reported by Lehn et al. and containing two μ_3-OH capping ligands[20] undergoes reversible, stepwise deprotonation to the corresponding $Cu_3(\mu_3\text{-O})_2$ species, which has not been structurally characterized. However, the μ_3-O caps of the latter are required for stereochemical reasons to remain pyramidal. Some trimeric Cu^{II} complexes with a $Cu_3(\mu_3\text{-O})$ core, reported to undergo both reversible protonation and electrochemical one-electron oxidation to their mixed-valent $Cu^{II}_2Cu^{III}$ analogues, have not been structurally characterized in either form.[22a−c] A related, also mixed-valent, $Cu^{II}_2Cu^{III}$ complex, containing two oxo caps, $Cu_3(\mu_3\text{-O})_2$, differs from

(12) Bencini, A.; Gatteschi, D. *EPR of Exchange Coupled Systems*; Springer: Berlin, 1990.
(13) Jones, D. H.; Sams, J. R.; Thompson, R. C. *J. Chem. Phys.* **1983**, *79*, 3877.
(14) Boča, R. *Program POLYMAGNET-99*; Slovak Technical University: Bratislava, Slovakia, 1999.
(15) Boča, R.; Baran, P.; Dlháň, L.; Hvastijová, M.; Wltschek, G. *Chem. Phys. Lett.* **1998**, *284*, 254.
(16) (a) Ardizzoia, G. A.; Cenini, S.; La Monica, G.; Masciocchi, N.; Maspero, A.; Moret, M. *Inorg. Chem.* **1998**, *37*, 4284. (b) Ehlert. M. K.; Rettig, S. J.; Storr, A.; Thompson, R. C.; Trotter, J. *Can. J. Chem.* **1992**, *70*, 2161. (c) Ehlert. M. K.; Rettig, S. J.; Storr, A.; Thompson, R. C.; Trotter, J. *Can. J. Chem.* **1990**, *68*, 1444. (d) Raptis, R. G.; Fackler, J. P., Jr. *Inorg. Chem.* **1988**, *27*, 4179. (e) Murray, H. H.; Raptis, R. G.; Fackler, J. P., Jr. *Inorg. Chem.* **1988**, *27*, 26.
(17) (a) Ardizzoia, G. A.; Cenini, S.; La Monica, G.; Masciocchi, N.; Moret, M. *Inorg. Chem.* **1994**, *33*, 1458. (b) Raptis, R. G.; Murray, H. H., III; Fackler, J. P, Jr. *J. Chem. Soc., Chem. Commun.* **1987**, 737.
(18) Virovets, A. V.; Podberezskaya, N. V.; Lavrenova, L. G. *J. Struct. Chem.* **1997**, *38*, 440.
(19) Meenakumari, S.; Chakravarty, A. R. *J. Chem. Soc., Dalton Trans.* **1992**, 2305.
(20) Comarmond, J.; Dietrich, B.; Lehn, J.-M.; Louis, R. *J. Chem. Soc., Chem. Commun.* **1985**, 74.
(21) Ho, D. M.; Bau, R. *Inorg. Chem.* **1983**, *22*, 4079.
(22) (a) Datta, D.; Chakravorty, A. *Inorg. Chem.* **1983**, *22*, 1611. (b) Datta, D.; Chakravorty, A. *Inorg. Chem.* **1982**, *21*, 363. (c) Datta, D.; Mascharak, P. K.; Chakravorty, A. *Inorg. Chem.* **1981**, *20*, 1673. (d) Ross, P. F.; Murmann, R. K.; Schlemperer, E. O. *Acta Crystallogr.* **1974**, *B30*, 1120. (e) Beckett, R.; Hoskins, B. F. *J. Chem. Soc., Dalton Trans.* **1972**, 291.

2 in the pyramidal geometry of its O atoms.[23] Approximately planar $Cu_3(\mu_3\text{-O})$ groups, with Cu−O−Cu angles in the 113(2)−119(2)° range, have been found in the structure of a hexanuclear carboxylato cluster containing H-bonded μ_3-O and μ_3-OH ligands with the proton crystallographically disordered between the two sites, as well as in a similar dimer-of-trimers oximato complex.[24] The X-ray crystal structures of **1a,b** and **4** are in agreement with those of the aforementioned related complexes containing the $Cu_3(\mu_3\text{-OH})$ moiety. In contrast, the structural characterization of **2** adds a new motif—the hitherto unknown, but anticipated,[25] planar $Cu_3(\mu_3\text{-O})$ unit—to the diverse chemistry of divalent copper. Unlike copper, this is a common motif in the chemistry of 3d- and 4d-transition-metal−carboxylato trimers of the type $[M_3(\mu_3\text{-O})(\mu\text{-OCOR})_6L_3]$.[26] As the copper d orbitals of appropriate symmetry to accept back-donation of electrons from the filled oxygen p_z orbital (perpendicular to the Cu_3O plane) are already occupied, the reason for the planarity of the $Cu_3(\mu_3\text{-O})$ unit of **2** cannot be other than the minimization of the Cu−O bond lengths. The coordinative unsaturation of the square-planar Cu^{II} centers corroborates this argument. Obviously, the formation of the planar $Cu_3(\mu_3\text{-O})$ motif and the crystal lattice energy of **2** are significant enough to offset the deprotonation of the μ_3-OH group; the proton affinity of oxide ion is −554.3 kcal/mol, compared with −403.6 kcal/mol for hydroxide.[27]

The approximate 3-fold symmetry of **2** is also worth noting. While the ^{1}H NMR spectra of all three compounds **1**−**3** are consistent with 3-fold average molecular symmetry in solution, the crystallographically characterized solid-state symmetries of **1** and **3** deviate significantly from ideal C_{3v} and D_{3h}, respectively. Such deviations, through a Jahn−Teller distortion, are common in tricopper systems to avoid the spin-frustrated state dictated by strict 3-fold symmetry.[28] These distorted complexes are typically antiferromagnetically coupled, $S = 1/2$ systems. In contrast, **2** deviates only slightly from 3-fold symmetry even in the solid state, and this, along with the novelty of its planar $Cu_3(\mu_3\text{-O})$ core, prompted us to investigate its magnetic properties. While the antiferromagnetic coupling of three Cu atoms of **2** is not surprising, the magnitude of this coupling, $J_{Cu-Cu} = -500$ cm^{-1}, is much more negative than the −23 and −148 cm^{-1} values reported for the related complex $Cu_3(\mu_3\text{-OH})(\mu\text{-Cl})(\mu\text{-pz})_3(py)_2Cl$ with Cu−Cu distances of 3.112(1)−3.321(1) Å.[5b] As the Cu−Cu distances of **2**, 3.269(1) and 3.287(1) Å, fall into the same range, its more negative J_{Cu-Cu} can be attributed to the better communication among the spin-carrying $d_{x^2-y^2}$ orbitals of the three copper atoms through their coplanar p_x and p_y oxygen orbitals of μ_3-O than through the corresponding out-of-plane orbitals of pyramidal μ_3-OH. Since the $[Cu(\mu\text{-pz})]_3$ frames of the μ_3-OH and μ_3-O species are practically identical, the role of the μ-pz groups, which are known mediators of antiferromagnetic exchange,[29] is a common factor in complexes **1** and **2** and has, therefore, been omitted in the comparison of their Cu−Cu coupling pathways. The dependence of J_{Cu-Cu} on the Cu−O−Cu angle in dimeric and trimeric complexes is well established in the literature[1b,e,30] and has recently been observed in a related system.[1c] An even more negative J value of ∼−1000 cm^{-1} has been measured in a hexanuclear complex containing two approximately planar $Cu_3(\mu_3\text{-O})$ groups with Cu−O bond lengths in the range of 1.854(2)−1.890(2) Å.[1e] The local maximum of the magnetic susceptibility of **2** at about 50 K is probably caused by some minor structural change of the complex, such as twisting of the $[Cu(\mu\text{-pz})]_3$ metallacycle, or freezing of the dynamic Jahn−Teller distortion.

There are a few examples of Cu^I complexes containing a $Cu_3(\mu_3\text{-Cl})_2$ group in the literature, but none of Cu^{II}.[31] In those Cu^I cases, as well as in the Cu^{II} complexes **3a,b** described here, the chlorides are loosely held to the Cu trimer at a wide range of distances—2.407(7)−2.678(8) Å for Cu^I and 2.341(2)−3.056(2) Å for **3a,b**—indicating that crystal packing forces influence their positions.

Related to **1**−**3** are some known copper(I), $[Cu(\mu\text{-pz*})]_3$, complexes of substituted pyrazole ligands (pz* = 3,5-R_2-pz; R = Me, Ph).[32] Interestingly, no trimeric Cu^{II} counterparts of the latter are known to date. In molecular modeling studies of such hypothetical Cu^{II} trimers, we found that structures analogous to those of **2** and **3** are hindered by steric repulsions between the chloride ligands and the alkyl/aryl groups at the μ-pz* 3- and 5-positions. On the other hand, the copper(I)−pyrazolato complex $[Cu(\mu\text{-pz})]_n$ of the parent unsubstituted pyrazole is a long-known, recently structurally characterized, one-dimensional polymer.[33] A Cu trimer, able to cycle between the Cu^I_3 and Cu^{II}_3 through the intermediate mixed-valent states, might model the structure or mimic the activity of tricopper oxygenases. Such a currently unavailable catalytic system may be accessible by using different, appropriately substituted pyrazoles.

The terminal chloride ligands of **1** and **2** are readily substituted by neutral or other anionic ligands in metathetical reactions with sodium or silver salts, and trimeric complexes containing terminal bromide, isocyanate, carboxylate anions, or neutral thf and pyrazole ligands have been characterized.

(23) Cole, A. P.; Root, D. E.; Mukherjee, P.; Solomon, E. I.; Stack, T. D. P. *Science* **1996**, *273*, 1848.
(24) (a) Wang, S.; Pang, Z.; Zheng, J.-C.; Wagner, M. J. *Inorg. Chem.* **1993**, *32*, 5875. (b) Curtis, N. F.; Gladkikh, O. P.; Heath, S. L.; Morgan, K. R. *Aust. J. Chem.* **2000**, *53*, 577.
(25) Singh, K.; Long, J. R.; Stavropoulos, P. *Inorg. Chem.* **1998**, *37*, 1073.
(26) Cannon, R. D.; White, R. P. *Prog. Inorg. Chem.* **1988**, *36*, 195.
(27) Hopkinson, A. C.; Holbrook, N. K.; Yates, K.; Csizmadia, I. G. *J. Chem. Phys.* **1968**, *49*, 3596.
(28) (a) Kahn, O. *Chem. Phys. Lett.* **1996**, *265*, 109. (b) Clérac, R.; Cotton, F. A.; Dunbar, K. R.; Hillard, E. A.; Murillo, C. A.; Petrukhina, M. A.; Smucker, B. W. *Chemistry* **2001**, *4*, 315.
(29) Berends, H. P.; Stephan, D. W. *Inorg. Chem.* **1987**, *26*, 749.
(30) Ruiz, E.; Alemany, P.; Alvarez, S.; Cano, J. *J. Am. Chem. Soc.* **1997**, *119*, 1297.
(31) (a) Bresciani, N.; Marsich, N.; Nardin, G.; Randaccio, L. *Inorg. Chim. Acta* **1974**, *10*, L5. (b) Ellermann, J.; Knoch, F. A.; Meier, K. J. *Z. Naturforsch.* **1990**, *45b*, 1657. (c) Colacio, E.; Cuesta, R.; Moreno, J. M. *Inorg. Chem.* **1997**, *36*, 1084.
(32) (a) Ardizzoia, G. A.; Cenini, S.; La Monica, G.; Masciocchi, N.; Maspero, A.; Moret, M. *Inorg. Chem.* **1998**, *37*, 4284. (b) Ehlert, M. K.; Rettig, S. J.; Storr, A.; Thompson, R. C.; Trotter, J. *Can. J. Chem.* **1992**, *70*, 2161. (c) Ehlert, M. K.; Rettig, S. J.; Storr, A.; Thompson, R. C.; Trotter, J. *Can. J. Chem.* **1990**, *68*, 1444. (d) Raptis, R. G.; Fackler, J. P., Jr. *Inorg. Chem.* **1988**, *27*, 4179.
(33) (a) Okkersen, H.; Groeneveld, W. L.; Reedijk, J. *Recueil* **1973**, *92*, 945. (b) Masciocchi, N.; Moret, M.; Cairati, P.; Sironi, A.; Ardizzoia, G. A.; La Monica, G. *J. Am. Chem. Soc.* **1994**, *116*, 7668.

However, precipitation of chlorides in the absence of appropriate coordinating ligands leads to trimer ring-opening reactions with products of larger nuclearity. Precipitation of the bridging chlorides of **3** allows the introduction of new triply bridging ligands, such as alkoxides, to this system. Those results will be reported elsewhere.

Supporting Information Available: X-ray crystallographic files in CIF format for **1a**, **1b**, **2**, **3a**, **3b**, and **4** and an ORTEP drawing with the labeling scheme of **3a**. This material is available free of charge via the Internet at http://pubs.acs.org.

IC010670L